Resilient Cities and Structures 1 (2022) 1–12

Contents lists available at ScienceDirect

Resilient Cities and Structures

journal homepage: www.elsevier.com/locate/rcns

Seismic resilience of building inventory towards resilient cities

Juan Gustavo Salado Castillo[a,*], Michel Bruneau[b], Negar Elhami-Khorasani[b]

[a] Technological University of Panama, Panama, Panama
[b] University at Buffalo, State University of New York, Buffalo, United States

ARTICLE INFO

Keywords:
Seismic resilience
Building resilience index
Community
Repair cost
Occupancy level
Asset value

ABSTRACT

Resilience of a community after an extreme event depends on the resilience of different infrastructure including buildings. There is no well-established approach to characterize and integrate building resilience for community-level applications. This paper investigates how different potential functionality measures can be used to quantify building resilience indexes, and how the results could be aggregated for a set of buildings to provide an indicator for the resilience of an entire community. The quantification of building resilience is based on different functionality measures including repair cost, occupancy level, and asset value. An archetype city block with four different buildings is defined. The individual results for each building are combined using a weight-based approach to quantify the resilience index for the city block. The study then considers small-scale communities with different number of buildings to investigate the influence of contractor availability and collapse probability on the resilience indexes for the set of buildings. Both parameters are shown to be important when quantifying the resilience index. It is also demonstrated that the overall resilience of a community is directly influenced by the resilience of individual buildings. The findings presented here are useful both from the perspective of quantifying the resilience of a community on the basis of its building inventory, as well as for possible inclusion into a holistic framework that aims to quantify community resilience.

Introduction

The research on resilience from an engineering point of view has been growing. Nearly two decades ago, the term “community seismic resilience”, together with a framework to quantify it, was first defined [1]. The majority of research works on this topic have focused on lifelines and networks (e.g., electricity, gas or services provided to customers) [2] or on overall frameworks to integrate physical, social, and economic factors (e.g., [3–6]). It is recognized that quantifying resilience is a multidisciplinary problem [7], and software platforms, such as HAZUS [8] and IN–CORE [9], have been developed to perform resilience assessment of communities. These tools rely on an extensive set of fragility functions for a range of elements or components, for different types of buildings and infrastructure networks (e.g., [10,11]), to quantify consequences of damage in terms of losses.

While much has been studied in the perspective of overall community resilience [12–14], it remains that resilience of the building inventory is key to resume functionality in a community. Despite progress made so far, there is still a need to define proper functionality measures, quantify resilience for buildings, and aggregate the functionality of individual buildings for a community level assessment [3]. When quantifying building resilience, one essential consideration is that both structural and non-structural elements in buildings are susceptible to damage, and therefore, they both should be included in the assessment [15]. Evaluating damage in structural and non-structural components can be achieved using engineering parameters, but how that damage is translated to a measure of functionality still poses a challenge for the purpose of resilience quantification [16]. Several frameworks have been developed to generically quantify resilience for individual buildings (e.g., [4,5]); others have attempted the quantification of resilience using engineering parameters either for individual buildings or systems (e.g., [17,18]).

The work presented here aims to integrate the resilience indexes of individual buildings to obtain an indicator for the resilience of an archetype city block, and expand the concept for application to a community. Resilience indexes for the individual buildings are obtained using the functionality measures defined in [19]. Sensitivity of the resilience index to contractor availability and the probability of collapse for communities with different number of buildings is investigated. An approach is proposed to aggregate and communicate the resilience of building inventory within a community.

* Corresponding authors.
E-mail address: juan.salado1@utp.ac.pa (J.G. Salado Castillo).

https://doi.org/10.1016/j.rcns.2022.03.002
Received 5 January 2022; Received in revised form 19 March 2022; Accepted 19 March 2022

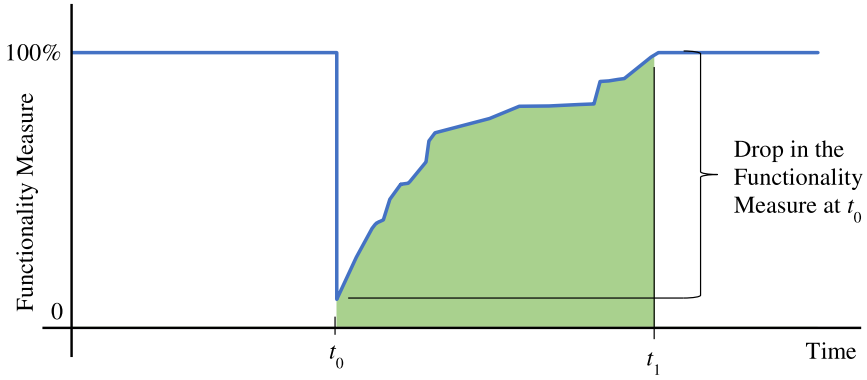

Fig. 1. Measure of seismic resilience.

Theoretical background and study setup

Resilience concept

To quantify resilience, the area under a curve, with the vertical axis as a functionality measure and the horizontal axis as time, can be computed. For example, in Fig. 1, the measure of resilience can be obtained by calculating the area between the times t_0 and t_1. It can be observed that at time t_0, there is a sudden drop in functionality, as a reflection of the instantaneous damage that is typically produced by an earthquake (which is the case at hand) [1]. The rate of this drop in functionality can differ for other hazards. In modern societies, functionality is progressively regained as part of the post-earthquake recovery process beyond time t_0 and the initial functionality measure is ideally reached again at time t_1. Evidently, this is not always the case, as functionality can also reach a lower or a higher level than the initial value [20], but that is a minor issue beyond the scope of this paper (with one exception described later).

Adopted buildings, methodologies, and scenarios

To determine how building resilience indexes can be used as an indicator for the resilience of an archetype city block, and expanded for the entire building inventory of a city, the resilience of individual buildings must first be calculated. Here, for illustration purposes, this was done using four buildings, arbitrarily selected to have different structural systems and characteristics. The buildings are a 3-story buckling-restrained braced (BRB) frame (Building (1)), a 4-story reinforced-concrete (RC) frame (Building (2)), a 2-story building with reinforced masonry (RM) walls (Building (3)), and another 2-story building but with unreinforced masonry (URM) walls (Building (4)). Together, they are considered here to define an archetype city block. A summary of some properties for the four example buildings is presented in Table 1, and additional properties and parameters used for the design can be found in [19]. The FEMA P-58 [21] methodology for the "Seismic Performance Assessment of Buildings" as implemented in the "Performance Assessment Calculation Tool (PACT)" [22] was used to obtain the resilience index for each of the above individual buildings.

Table 1
Summary of properties for the four buildings.

Building	Total Cost ($)	Average Number of Occupants	Total Area (sq. ft.)
Building (1) (3-story BRB frame)	38,850,000	69	78,700
Building (2) (4-story RC frame)	27,580,000	82	86,400
Building (3) (2-story RM)	6110,000	15	14,500
Building (4) (2-story URM)	8550,000	30	28,800
Total	81,100,000	196	208,400

Regarding the sequence of repair works, the FEMA P-58 [21] computes the total repair time based on the maximum number of workers per square foot that is defined in the Building Performance Model and assuming that the repair works can be performed in series or parallel. The repair strategies (i.e., series or parallel) are defined based on distribution of the repair works across floors. This means that the serial repair strategy considers a repair work sequence that proceeds floor-by-floor, while the parallel repair strategy considers simultaneous repair works on all floors. In FEMA P-58, it is acknowledged that neither repair strategies simulate a real repair sequence. A real representation of a repair schedule should consider that some repair works must be completed before others (e.g., fixing a pipe in a wall before fixing the wall), or that some repair works allow a higher number of workers on site than others (e.g., performing interior repairs over a wide area compared to fixing an elevator in a specific area/location/confined space).

The Downtime Assessment Methodology [23], incorporated in this paper, establishes typical Repair Sequences to address the limitation of the FEMA P-58 methodology regarding labor allocation and logic in the sequence of repair works. Once the average damage states for each component and floor are defined (obtained from the performance assessment), "Repair Classes" can be assigned using the classification provided in the Downtime Assessment Methodology. After the Repair Classes are defined, each component should be assigned a Repair Sequence that defines the order by which the various repair works are going to proceed. This classification determines which repair works can be performed simultaneously and which cannot. Also, the methodology dictates that repair works for non-structural components (Repair Sequences A to F in the methodology) should never start before repair works for structural components is completed, to guarantee occupant safety. The analysis also incorporated the Downtime Assessment Methodology [23] to account for delays (a.k.a. impeding factors) that can be incurred before the initiation of repair works, due to factors such as permitting, financing, inspections, and many others causes.

Two scenarios were defined to consider the effect of impeding factors, representing arbitrary best- and worst-case scenarios, referred here to as Option 1 (worst scenario) and Option 2 (best scenario). It is recognized that scenarios dramatically worse than the one considered here are possible, therefore, the two scenarios considered allow to assess to some degree the sensitivity of findings to the type of building (e.g., essential or non-essential), financial conditions, contractor and engineering availability, and Repair Classes. The same parameters used in [19] for each of the impeding factors were assumed here. An overview of the selected functionality measures will be presented in the next section; more details on the step-by-step methodology can be found in [19].

The simplified analysis procedures of FEMA P-58 were used to generate the demand input for the Building Performance Models, and generate the resilience curves for each building. Several spectral acceleration

(S_a) values, namely, 0.1 g, 0.5 g, 1.0 g, 1.5 g, and 2.0 g, were considered to obtain the resilience indexes for each building as a function of S_a. It should be noted that the same values of S_a were used for the four example buildings to have a comparable measure between the results in terms of resilience indexes. The results in the previous study by the authors [19] showed the importance of considering the collapse probability in defining the resilience indexes. Only one potential collapse mode, with complete failure in all floors in the building, is assumed here for simplicity. However, it should be noticed that buildings can also experience partial collapses, and this would result in different resilience indexes, but this consideration is beyond the scope of this work for the current purposes. Eq. (1) was used to compute the resilience index including the collapse probability:

$$RI = \frac{RI_{NC} * (NR - CR)}{NR} \quad (1)$$

where RI is the resilience index that considers collapse probabilities, RI_{NC} is the resilience index for cases that did not collapse (out of 500 realizations for the purpose of this study), NR is the number of realizations considered in the Building Performance Models (which is 500 for this case), and CR is the number of realizations that experienced collapse.

Approaches for resilience quantification

The resilience curve presented in Section 2.1 generically refers to a functionality measure, leaving it to the user to identify/define the type of functionality measure most suitable for the application at hand. For buildings, different approaches are possible. Here, three different functionality measures are used to calculate resilience, namely repair costs, occupancy levels, and asset values. The pros and cons of each approach have been presented elsewhere [19]; the focus here is on quantification of resilience at a larger scale by aggregating the results obtained for individual buildings, but a brief overview of each functionality measure follows to provide context and perspective on the broader results presented within the scope of this paper.

The first functionality measure uses the value of a building as a proxy for its functionality, by computing the repair costs required to return the building to its pre-earthquake condition (this idea was first proposed by [4]). The costs used here are obtained from the PACT software, together with the estimated time required to perform those repair works. The concept used to define functionality measure based on repair cost is presented in Fig. 2(a). Three points can be observed: point A corresponds to the drop in functionality (analogous to what was presented in Fig. 1), and in this case, represents the total cost of the damage, and likewise the cost to repair the building. Based on the nature of the seismic event, and as addressed by the Downtime Methodology [23], a downtime due to impeding factors is included before the initiation of the repair works in the examples considered. This downtime ends at point B, which marks the initiation of the repair works in the building, and consequently, the beginning of the recovery in functionality. Once all the repairs are concluded (point C), the building is back to its identical pre-earthquake condition.

The second approach uses building occupancy to measure functionality. The occupancy type for the four buildings is considered as “commercial offices”, and the percentage of employees able to return to their workplaces is defined as the functionality measure. Return to workplace is grouped into three categories: Re-Occupancy (50% of the total normal occupancy level), Functional Recovery (adding an additional 40% of the total normal occupancy level) and Full Recovery (return to 100% total normal occupancy level), corresponding to the completion of repair works for Repair Classes 3, 2 or 1, respectively. As defined in the Downtime Assessment Methodology [23], for both structural and non-structural components, a Repair Class 3 is assigned to components with enough damage to represent a life-safety hazard, a Repair Class 2 to components that hinder functionality, and a Repair Class 1 to components with cosmetic damage. Similar to the repair cost approach, Fig. 2(b) for the occupancy level approach shows a time duration of t_1 representing the downtime due to impeding factors. This is followed by a time interval of t_2 required to repair the building, beyond which the building operates at full functionality. The time interval t_3 shown on the figure is used to define a reference time for resilience calculations. For example, if a building suffers a 50% reduction in the functionality measure (e.g., occupancy level), and the repair works require 1 day to be completed, the resilience index (without considering a reference time) will be 50%. If another building suffers the same reduction in functionality, but requires 2 days to be repaired, the resilience index is the same (50%). However, it is clear that the first building in this example is more “resilient” than the second one, because it returns to the original functionality in a shorter time. Hence, the inclusion of the variable t3 to use a reference time of 2 days for both buildings, leads to a resilience index of 75% for the first building, which is higher than the resilience index of 50% for the second building.

The third functionality measure considered is the asset value. Asset value is defined here by combining property value and property income. The definition of property value is consistent with the concept explained for the repair cost approach (i.e., the building value before the drop due to earthquake damage in Fig. 2(a)). The property income corresponds to the difference between the gross income that the property generates (e.g., by leasing available spaces, and obtained from a real estate website [24] for the building location) and the building’s maintenance and

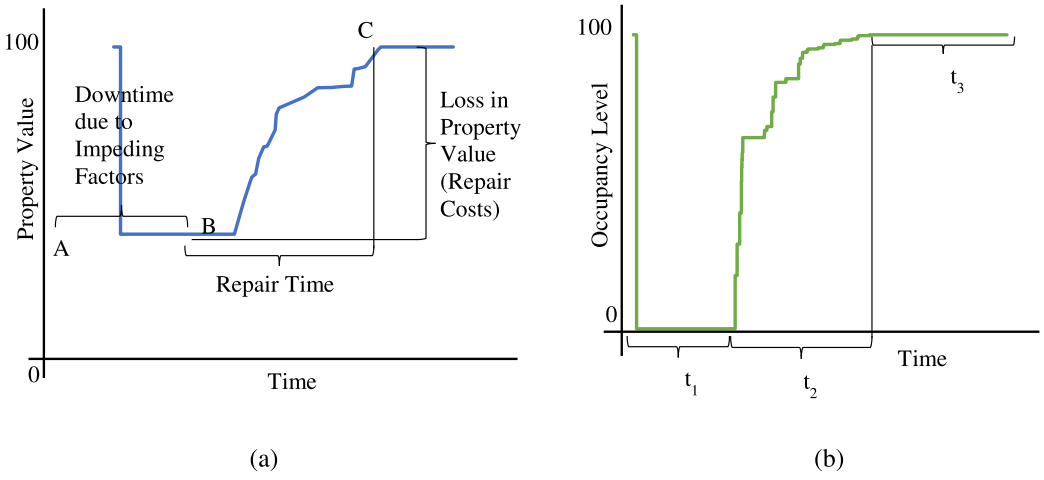

Fig. 2. Concept curves for the quantification of seismic resilience based on: (a) repair cost and (b) occupancy level.

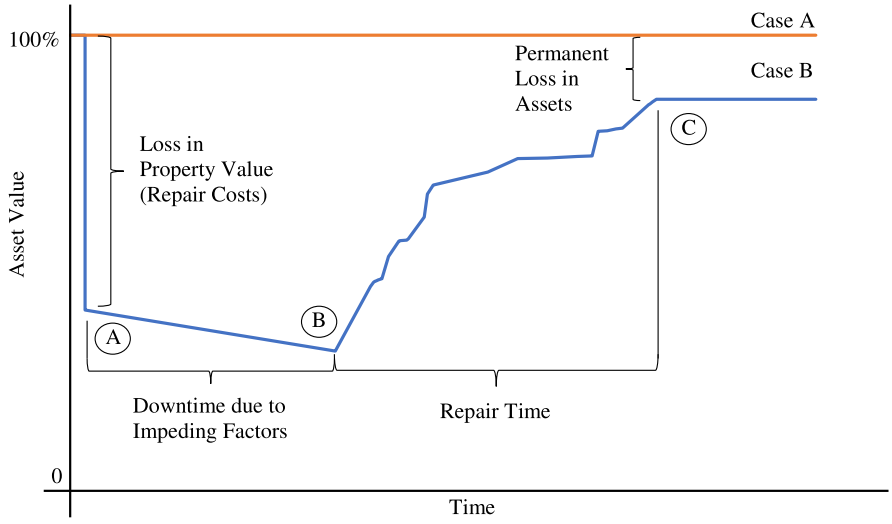

Fig. 3. Concept curve for the quantification of seismic resilience based on asset values, considering both property value and property income.

operations costs (e.g., utilities, loan payments, etc.). It is assumed that in worst case scenario, both incomes and expenses are the same, meaning that the property does not generate any profit (Case A in Fig. 3) – which effectively normalizes the functionality to a constant basis in the absence of earthquakes. However, in the case of an earthquake, there is a loss in property value, that must be recovered through repair works to return the building to its pre-earthquake condition (point A in Fig. 3). Similar to the two previous approaches, a downtime due to impeding factors is considered after the earthquake occurrence. However, in this approach, the functionality measure continues decreasing during the downtime, as a result of the loss in income. At point B in Fig. 3, the repair works begin, and both property value and income start increasing. The increase in income is defined using the same percentages for re-occupancy of the buildings defined for the occupancy level approach (i.e., based on the completion of repair works for each Repair Class, and in this case, per floor). Note that the rate of income recovered is less than that prior to the earthquake until the building is fully leased again. Repair works conclude at point C in Fig. 3, but contrary to the two previous approaches, in this case the functionality measure does not return to its initial value, as a result of the loss in income from the time of earthquake occurrence until completion of repair works.

Summary of resilient indexes for the four example buildings

The resilience indexes obtained for the four example buildings and both options considered are presented in Tables Table 2 to Table 4. Table 2 corresponds to the resilience indexes for the repair cost approach, Table 3 presents the resilience indexes for the occupancy level approach, and Table 4 presents the resilience indexes for the asset value approach. Five different S_a values were considered, and the listed indexes include probability of collapse for each building, computed using Eq. (1). The resilience indexes are expected to decrease as S_a increases, considering that the probability of collapse increases. Additionally, for a fair comparison of resilience indexes between the buildings, the reference time that is used to calculate the resilience index (t_3 in Fig. 2(b)) should be taken as the longest required repair time to achieve full re-occupancy between Options 1 and 2 for all the example buildings and for all the considered S_a values (which is 525 days for Building (1) Option 1 with an S_a of 2.0 g).

Methodology for quantification of seismic resilience for a city block

Weight-based approach

Having resilience results for individual buildings, it is then possible to compute the combined resilience of an inventory of buildings. For this purpose, here, an archetype city block is defined consisting of the four buildings mentioned in Section 2.2. As a crude estimate, the mean value of the resilience indexes for the four buildings could be used as an indicator for the resilience of the city block. However, this mean resilience index for the archetype city block would ignore the fact that a particular building can have a dominant impact on the resilience of the city block. A similar argument can be made about the median value (particularly so in this example, since the median in this case is the average of the two intermediate values).

The contribution of each building to the resilience index of the archetype city block can vary as a function of its individual properties. For this purpose, a relevant building property (from Table 1) was identified for each of the three approaches considered, namely, the repair cost,

Table 2
Resilience indexes based on repair costs and as a function of S_a.

S_a (g)	Building (1)		Building (2)		Building (3)		Building (4)	
	Opt. 1 (%)	Opt. 2 (%)	Opt. 1 (%)	Opt. 2 (%)	Opt. 1 (%)	Opt. 2 (%)	Opt. 1 (%)	Opt. 2 (%)
0.1	99.4	99.7	99.2	99.7	100.0	100.0	97.8	97.8
0.5	92.6	96.8	94.5	97.1	66.7	67.2	27.3	27.8
1.0	86.8	92.7	80.9	85.5	16.7	16.9	4.0	4.1
1.5	72.8	78.3	62.8	67.4	4.9	5.0	0.4	0.4
2.0	52.4	56.3	48.7	52.6	0.0	0.0	0.4	0.4

Table 3
Resilience indexes based on occupancy level and as a function of S_a.

S_a (g)	Building (1)		Building (2)		Building (3)		Building (4)	
	Opt. 1 (%)	Opt. 2 (%)	Opt. 1 (%)	Opt. 2 (%)	Opt. 1 (%)	Opt. 2 (%)	Opt. 1 (%)	Opt. 2 (%)
0.1	59.3	84.4	59.4	84.5	100.0	100.0	97.8	97.8
0.5	43.7	76.8	49.0	79.9	40.3	57.4	16.7	23.8
1.0	36.7	69.2	43.0	64.0	10.1	14.3	2.6	3.5
1.5	29.0	56.6	33.7	46.8	3.0	4.2	0.3	0.3
2.0	20.8	40.7	25.2	35.5	0.0	0.0	0.2	0.3

Table 4
Resilience indexes based on asset values and as a function of S_a.

S_a (g)	Building (1)		Building (2)		Building (3)		Building (4)	
	Opt. 1 (%)	Opt. 2 (%)	Opt. 1 (%)	Opt. 2 (%)	Opt. 1 (%)	Opt. 2 (%)	Opt. 1 (%)	Opt. 2 (%)
0.1	97.6	99.0	96.5	98.5	100.0	100.0	97.8	97.8
0.5	92.0	96.1	91.6	95.8	65.3	66.7	26.5	27.5
1.0	85.8	91.5	78.6	83.8	16.3	16.7	3.9	4.1
1.5	71.7	77.1	61.6	66.0	4.8	4.9	0.4	0.4
2.0	51.6	55.5	47.8	51.5	0.0	0.0	0.4	0.4

Table 5
Weighting factors for the four buildings per considered approach.

Approach	Building (1)	Building (2)	Building (3)	Building (4)
Repair Costs	0.48	0.34	0.08	0.10
Occupancy Level	0.35	0.42	0.08	0.15
Asset Values	0.38	0.41	0.07	0.14

the occupancy level, and the asset value, to define weighting factors for the buildings when calculating the resilience index for the city block. For the repair cost approach, the total building price was defined as the most relevant property. Likewise, for the occupancy level approach, the average number of occupants was assumed as the most appropriate property. Finally, the total square footage for each building was identified as the most suitable property for the asset value approach, since it indirectly reflects income potential, building value, and occupancy. Using this information, weight factors (by which the resilience indexes for each building will be multiplied) are computed and presented in Table 5 for each of the four buildings and the three approaches considered.

Results for the archetype city block using the weight-based approach

Fig. 4 presents the resilience indexes for the archetype city block per S_a for both Options 1 and 2, using the weights presented in Table 5. For the repair cost approach, Option 2 presented higher resilience indexes than Option 1, but the difference between these options was narrow and did not exceed 6%. Given that Buildings (1) and (2) account for 82% of the total resilience index of the archetype city block, the low resilience indexes for Buildings (3) and (4) for high S_a, did not influence considerably the resilience index for the archetype city block. Additionally, an almost linear relationship between the resilience indexes and the S_a can be observed for this approach.

For the occupancy level approach, the resilience indexes for higher S_a are more affected by the percentage of collapse realizations than by the required repair time. As observed in Fig. 2(b), the resilience indexes obtained for the occupancy level approach are the lowest among the three approaches considered. This can be explained by the fact that the occupancy level penalizes the resilience index more than the other approaches when the building is not functional, that is the occupancy level is 0% during the downtime due to impeding factors and gradually increases to 100% at completion of the repair works.

Notable similarities are observed between the curves for the repair cost approach and the asset value approach. As was expected, lower resilience indexes were obtained in the asset value approach, but with differences in the resilience indexes between the repair cost and the asset value approaches that did not exceed 5%.

Sensitivity analyses on contractor availability and collapse percentage

Sensitivity analysis on contractor availability

The analysis presented for the four example buildings that form the archetype city block imposes limits on labor allocation according to the guidelines presented in the Downtime Assessment Methodology [23]. Those limits were established by the number of floors, square footage, and Repair Sequence. It was assumed that the maximum number of workers allowed by the considered limits would be available in the market to perform the repair works. However, it is expected that the required number of workers may not be available when a large number of buildings in a community experiences damage after an earthquake. Using the city block as a proxy for the building stock of an entire community to obtain city-level resilience index, the availability of contractors to perform all the needed repair works can turn into an issue that affects the resilience index for the community.

In order to study how contractor availability affects the resilience indexes for a set of buildings, a case study is performed by defining a city-block with a set of identical buildings. Fig. 5 shows the theoretical resilience curve for a building considering delays due to impeding factors and long-lead components. This curve starts with a drop in the functionality measure *FM* (i.e., repair costs, occupancy level, or asset values) in normal circumstances to a new αFM value after the earthquake. Following the initial drop, a delay by impeding factors defined as t_D is considered. From this point onward, an increase in the functionality measure obtained by repair works that did not require long-lead components is assumed. This increase is defined as h_1, or ωFM as a function of the original functionality measure, with the required completion time t_1. Following the increase in functionality, a delay is assumed due to long-lead components with the required time t_{LL}. Finally, the building returns to the initial functionality measure *FM*, where the increase in functionality is defined as h_2, or βFM as a function of the original functionality measure. The last recovery path corresponds to the repair works that require long-lead components. Also, it is assumed that this second increase in functionality is completed over time t_2. The total repair time t_R is defined as:

$$t_R = t_1 + t_{LL} + t_2 \tag{2}$$

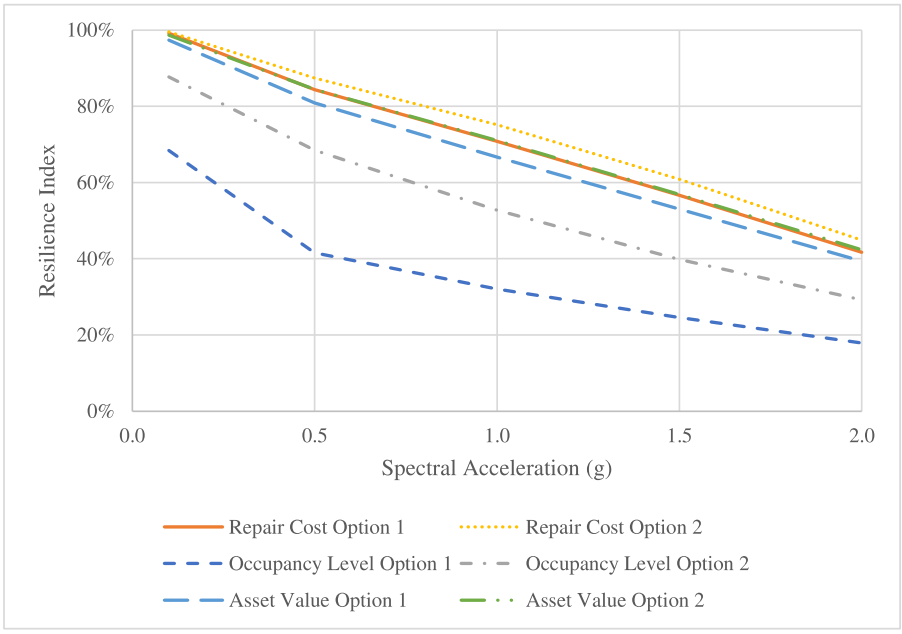

Fig. 4. Weight-based resilience indexes per S_a for the archetype city block.

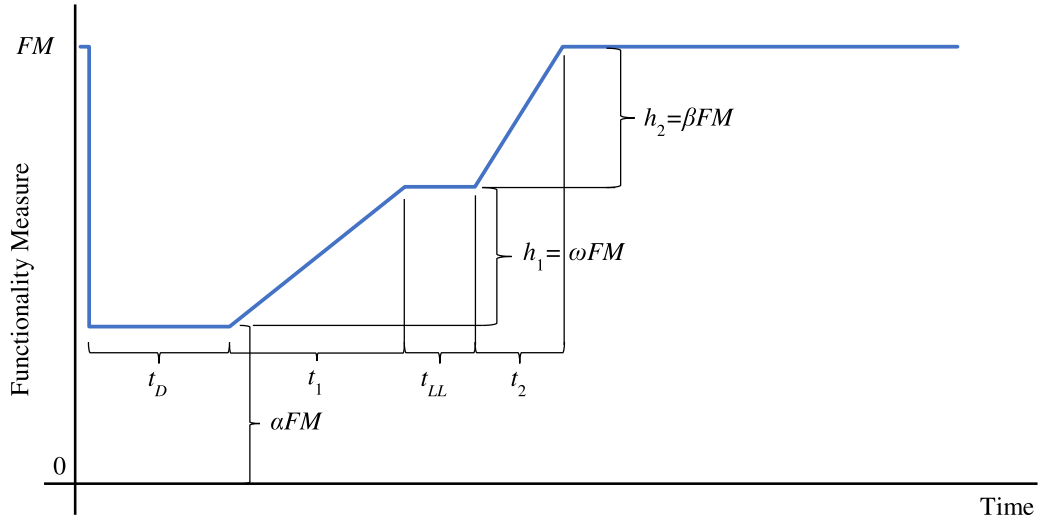

Fig. 5. Theoretical resilience curve for an example building.

It can be observed that α can be defined as:

$$\alpha = 1 - \omega - \beta \tag{3}$$

Using the weight approach presented in Section 3.1, and considering that there are no delays due to contractor availability, the resilience index for the archetype city block is equal to the resilience index for the example building, because all the buildings in the city-block are assumed to be identical (i.e., have the same weight factors) and work in all the buildings is performed in parallel (i.e., starting, progressing, and ending at the same time). The resilience index can then be defined as:

$$RI = \frac{\alpha\left(t_D + t_R\right) + \omega\left(0.5t_1 + t_{LL} + t_2\right) + 0.5\beta t_2}{t_D + t_R} \tag{4}$$

However, if there is only one contractor available to perform all the repair works, for the nth building in a set of m buildings, the repair works are delayed by an additional nt_R. For example, if two buildings require repairs, the term t_R (in both the numerator and the denominator) in Eq. (4) must be multiplied by a factor of 2 for the resilience index of the second building (while for the first building, the resilience index remains computed using the same as Eq. (4)). Each resilience index for a building must be computed considering the time lapse from the earthquake occurrence (i.e., the time at the drop in functionality in Fig. 5) to the completion of repair works for that building. Therefore, for the nth building, the resilience index is defined as:

$$RI = \frac{\alpha\left(t_D + nt_R\right) + \omega\left(0.5t_1 + t_{LL} + t_2\right) + 0.5\beta t_2}{t_D + nt_R} \tag{5}$$

Then, for the set of m buildings, the resilience index is defined as:

$$RI = \frac{1}{m}\sum_{n=1}^{m} \frac{\alpha\left(t_D + nt_R\right) + \omega\left(0.5t_1 + t_{LL} + t_2\right) + 0.5\beta t_2}{t_D + nt_R} \tag{6}$$

Fig. 6 presents the resilience indexes for the set of m buildings and for different values of m, ω, and β. The value of t_D was taken as 80 days for all the curves presented in Fig. 6. Table 6 lists the values assumed for t_1, t_{LL}, and t_2, and the value for t_R was computed using Eq. (2). The values of t_D, t_{LL}, t_1, t_2, β, and ω were arbitrarily assumed, but they are

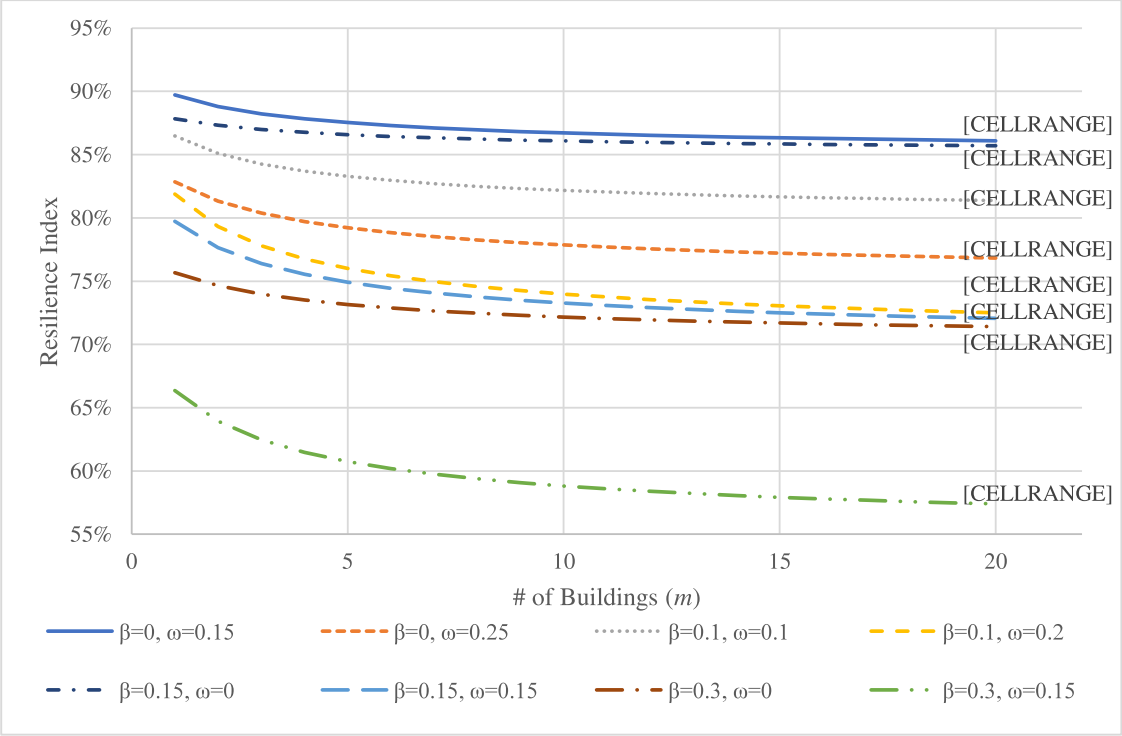

Fig. 6. Resilience indexes for a set of m buildings and different β and ω values.

Table 6
t_{LL}, t_1, t_2, and t_R for the different β and ω values.

	β=0.00, ω=0.15, α=0.85	β=0.00, ω=0.25, α=0.75	β=0.10, ω=0.10, α=0.80	β=0.10, ω=0.20, α=0.70	β=0.15, ω=0.00, α=0.85	β=0.15, ω=0.15, α=0.70	β=0.30, ω=0.00, α=0.70	β=0.30, ω=0.15, α=0.55
t_{LL}	0	0	35	35	35	35	35	35
t_1	135	135	135	135	0	135	0	135
t_2	0	0	70	70	70	70	70	70
t_R	135	135	240	240	105	240	105	240

based on the values and results obtained for the four example buildings presented earlier in the work. These assumptions serve the purpose of providing an example of the proposed methodology proposed to compute resilience indexes for a city block. The computed values for α using Eq. (3) are also indicated in the plot for each curve. The value of α provides a measure of how "functional" is the building immediately after an earthquake (refer to Fig. 5). It is important to recall that for the three approaches developed in this work (i.e., the repair cost, the occupancy level, and the asset value approaches), the value of α was higher for the repair cost and the asset value approaches than for the occupancy level approach. Additionally, the curves presented in Fig. 6 consider that only one contractor is available to perform the repair works. However, these results can be interpreted for a different number of contractors. For example, the resilience indexes for 10 buildings with 2 available contractors to perform the repair works, will be the same as those for 5 buildings and 1 contractor, or 15 buildings and 3 contractors.

In Fig. 6, it can be observed that, the value of resilience indexes decreases at first for a small increase in the number of buildings but eventually converges to the value of α as the number of buildings increases. Mathematically, this is because the first term in Eq. (6) becomes dominant for high values of n, and therefore, the equation reduces to only the value of α. Physically, this means that as the number of affected buildings increases, the resilience index is dictated by the robustness of the set of buildings (i.e., a more robust building withstands an adverse event better, where a larger value of α corresponds to a lower initial loss of functionality), rather than the required time duration to return to the original functionality level. Additionally, as the drop in functionality increases (i.e., the value of α decreases), the resilience indexes presented higher variations as the numbers of buildings increased. This can be observed in Fig. 6, where the presented curves are clustered depending on the value of α, with lower resilience indexes as α decreases. Both observations suggest that the drop in the functionality measure influenced the resilience indexes for the archetype city block more than the total required time to complete the repairs for all the buildings. This reinforces the idea that mitigation is important to achieve higher resilience indexes (i.e., mathematically, high values of α govern the resilience calculation).

To investigate the effect of the delays by impeding factors (i.e., t_D), the resilience indexes were computed for the same m buildings and values of ω and β as above, but with $t_D = 0$ days. In this case, the same two sets of values for t_1, t_{LL}, and t_2 were considered. Similar to Fig. 6, the obtained resilience indexes sharing the same α values were clustered close together, and the resilience indexes converged to α for large values of m. Higher resilience indexes were observed for a small number of buildings assuming $t_D = 0$, compared to the curves in Fig. 6. As expected, this could be an indicator that the delay by impeding factors only affects the initial stages of the recovery process. For example, the resilience index decreases by 3% when m changes from 1 to 10 for a t_D of 80 days, $\beta = 0.00$, and $\omega = 0.15$, but for a t_D of 0 days, the resilience index decreases by 5.3%. For the same conditions of β and ω, the resilience index decreases by 0.6% when m changes from 10 to 20 for a

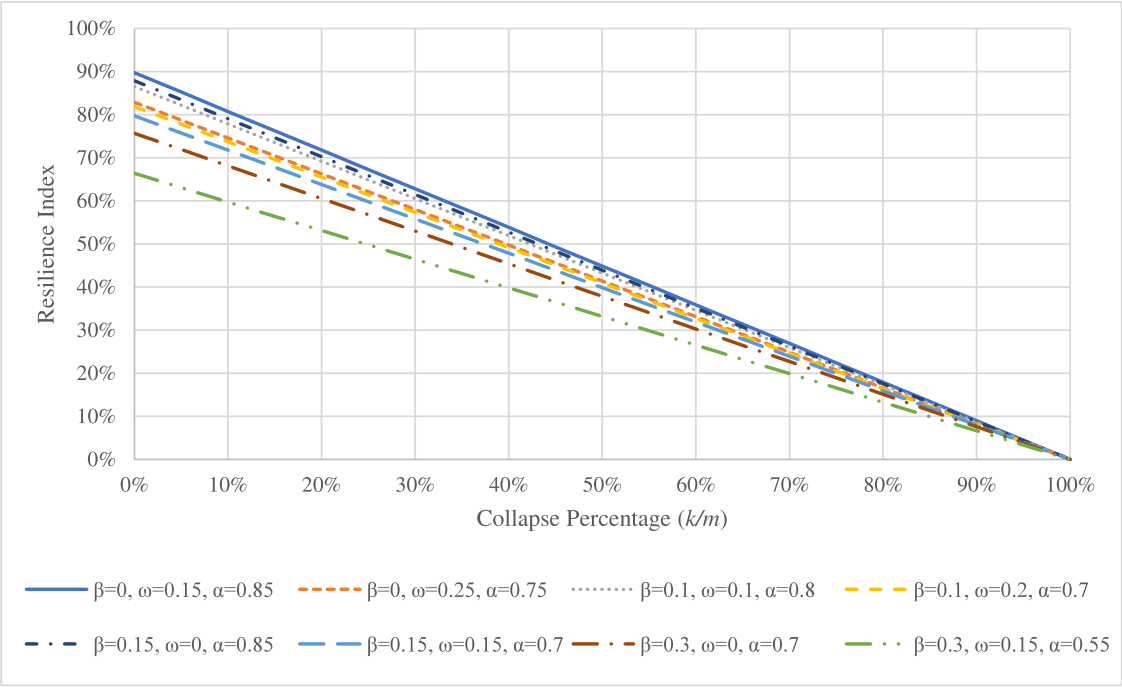

Fig. 7. Resilience indexes per collapse percentage for a set of m buildings and different β and ω values.

t_D of 80 days, and the resilience index decreases by 0.9% for a t_D of 0 days.

Sensitivity analysis on collapse percentage

The resilience indexes presented in Section 3.2 were based on the individual resilience indexes of each of the four example buildings (that were computed using individual collapse probabilities for each building). Following the same approach presented in Section 4.1, a framework to assess the influence of collapse probability on the resilience index of the archetype city block with a set of m buildings is presented here. In this case, for a building that collapsed, functionality remains zero for the entire time duration considered to reconstruct the building (which is longer than the time required to repair the affected buildings; i.e., $t_D + t_R$). For the buildings that did not collapse, the resilience curve is identical to the one presented in Fig. 5. Therefore, the resilience indexes for the buildings that collapsed is zero, and for the buildings that did not collapse is defined as in Equation 4.

If a set of m buildings consists of k buildings that collapsed, the resilience index for the archetype city block is defined as:

$$\boldsymbol{RI} = \left(1 - \frac{\boldsymbol{k}}{\boldsymbol{m}}\right)\left(\frac{\boldsymbol{\alpha}\left(\boldsymbol{t_D} + \boldsymbol{t_R}\right) + \boldsymbol{\omega}\left(0.5\boldsymbol{t_1} + \boldsymbol{t_{LL}} + \boldsymbol{t_2}\right) + 0.5\boldsymbol{\beta}\boldsymbol{t_2}}{\boldsymbol{t_D} + \boldsymbol{t_R}}\right) \quad (7)$$

Eq. (7) adjusts the resilience index of Eq. (4) to include the effect of collapsed buildings by multiplying the index with the percentage of buildings that did not collapse (where the term k/m represents the collapse percentage for the set of m buildings). Fig. 7 presents the resilience indexes for the set of m buildings with different collapse percentages and different values of β and ω. For all the curves presented in Fig. 7, it was assumed that t_D was 80 days, and t_1, t_{LL}, and t_2 are the same sets of values used in Section 4.1. The values computed for α using Eq. (3) are also the same as those in Section 4.1. All the curves presented in Fig. 7 converge to the same final point, which corresponds to a resilience index of 0 and a collapse percentage of 100%. Additionally, similar to Fig. 6, the curves are grouped close together based on the value of α, and the resilience indexes decrease as α decreases. This means that higher values of α led to higher resilience indexes. For brevity, the analysis for $t_D = 0$ is not presented here, as the effect of this parameter on the resilience index is similar to what was discussed in Section 4.1.

Sensitivity analysis on combination of contractor availability and collapse

This section studies the combined effects of the contractor availability (Section 4.1) and collapse (Section 4.2) on the resilience index for a set of m buildings by combining Eqs. 5 and 7. The combined analysis is evaluated for different values of m and for different values of β and ω. Two different collapse probabilities (where probability of collapse is defined as k/m) were considered for the set of buildings (namely, 10% and 20%).

Fig. 8 presents the percentage of buildings that have resilience indexes greater than or equal to different thresholds (namely, 75%, 70%, 65%, 60%, and 55%) for different values of m and collapse probabilities. For example, for a 10% collapse probability, the set of $m = 20$ has 30% of the buildings (i.e., 6 buildings) with a resilience index of 65% or greater. Similarly, for a 20% collapse probability, the set of $m = 50$ has 2% of the buildings (i.e., 1 building) with a resilience index of 65% of greater. In other words, this is the inverse cumulative distribution function (CDF) for the resilience index of the city block, considering different number of buildings and probability of collapse. The inverse CDF provides the probability that the buildings within the set will have a resilience index that is greater than or equal to the specified resilience index. For this analysis, the values of β and ω were assumed as 0.1 and 0.2, respectively ($\alpha = 0.7$). This means that the functionality measure drops to 70% of its initial value. Also, the values for t_D, t_{LL}, t_1, and t_2 were assumed as 80, 35, 135, and 70 days, respectively. It can be observed that, for a given probability of collapse, a city block with smaller number of buildings (lower values of m) has higher resilience indexes. As expected, lower values of m mean that the total required time to conclude all the repairs in the city block (i.e., $t_D + nt_R$) is shorter, and consequently, the resilience indexes were higher than those for a set with a larger value of m. Also, it can be observed that the set of curves for each collapse probability is only differentiated by a "shift", since the inclusion of collapse probability is linear (refer to Eq. (7)), and higher collapse probabilities mapped to lower resilience indexes (or, in other words, a shifting of the

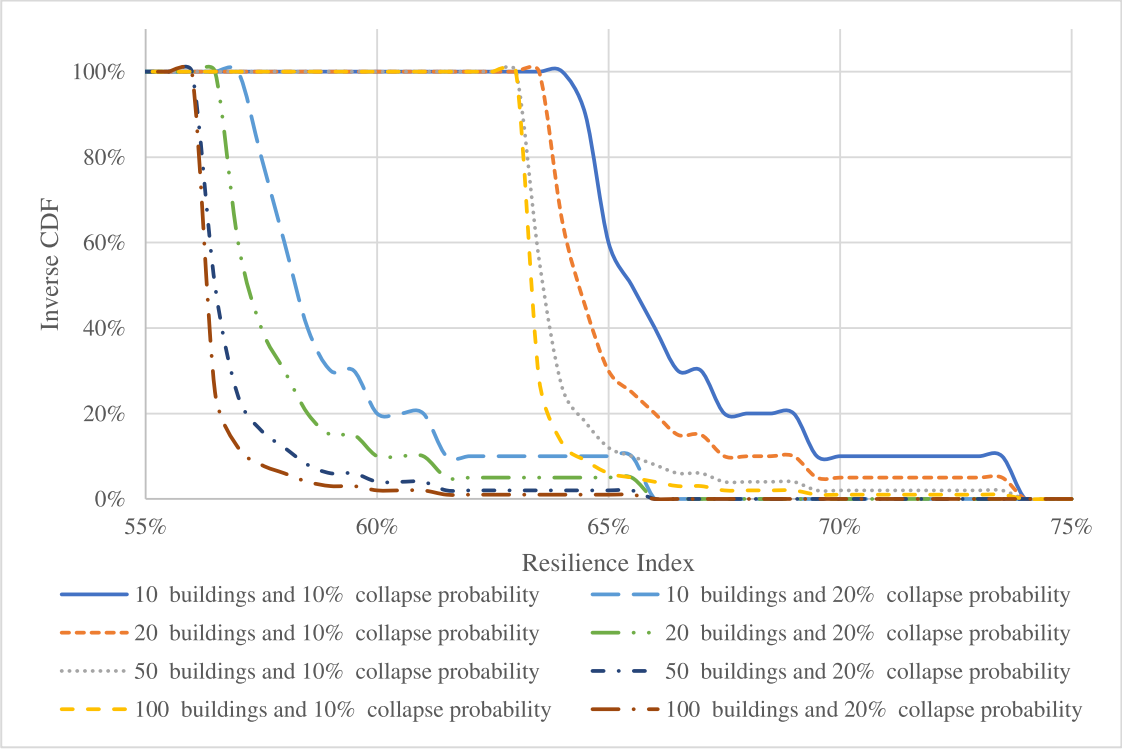

Fig. 8. Inverse CDF for the resilience indexes considering variation in the collapse probability (k/m) and number of buildings (m).

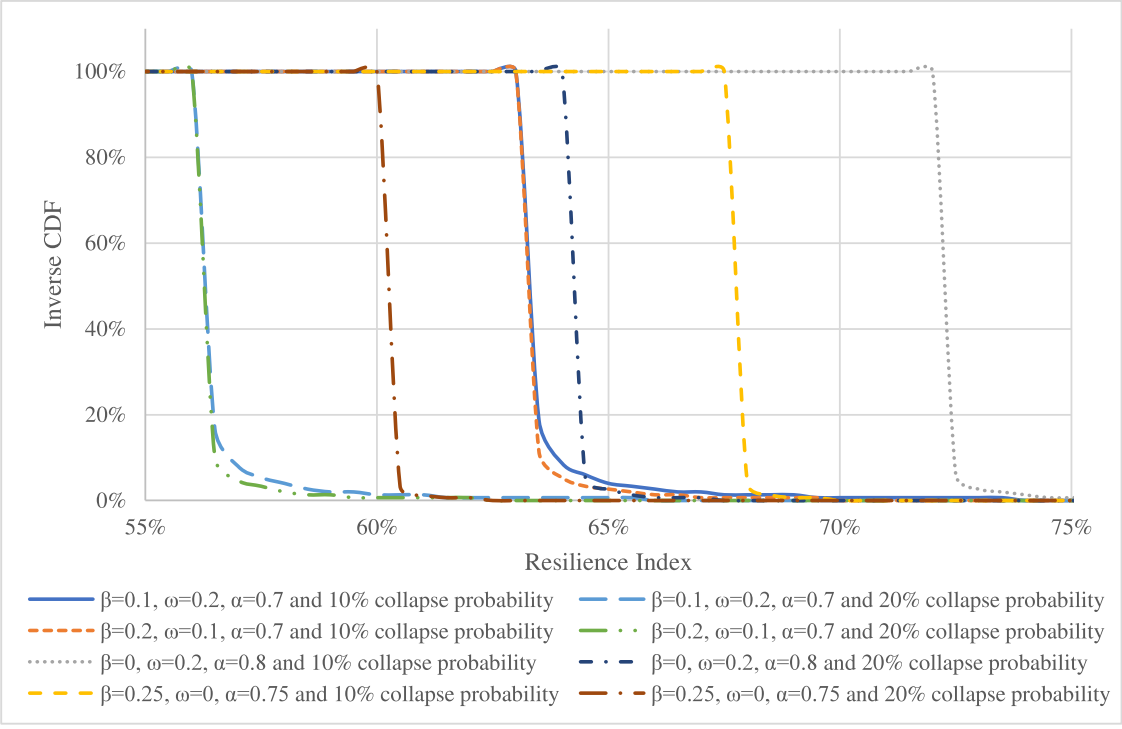

Fig. 9. Inverse CDF for the resilience indexes for a set of buildings (m = 150) considering variation in the collapse probability (k/m), β, and ω values.

same to the left). Additionally, the difference in the resilience indexes decreases as m increases, as was also observed in Fig. 6.

Fig. 9 presents the percentage of buildings that have resilience indexes greater than or equal to different thresholds (namely, 75%, 70%, 65%, 60%, and 55%) for different values of β and ω and collapse probabilities, for a community with 150 buildings. For example, for $\omega = 0.1$, $\beta = 0.2$ (i.e., α=0.70), and a 10% collapse probability, 2.7% of the buildings in the community have a resilience index of at least 65%. Similarly, for a 20% collapse probability, and the same values for ω and β, no building would achieve a resilience index of at least 65%, but 0.7% of the buildings in the community would achieve a resilience index of at least 60%. Again, this is the inverse CDF for the resilience index of

the city block, considering different values of β and ω, and probability of collapse. For all the curves presented in Fig. 9, t_D was 80 days and m was 150 (i.e., a community with 150 buildings). Two sets of values were assumed for t_1, t_{LL}, and t_2, and the value for t_R was computed using Eq. (2). Similar to Fig. 8, the curves obtained by varying the collapse probability are shifted versions of the curves having identical values of β and ω. Also, higher values of α present higher resilience indexes (curves more to the right). The fast drop from 100% to 0% in resilience index for lower values of α means that the difference in the resilience indexes between the first and the last repaired buildings is relatively small.

Community building-based resilience

Collapse correlation

For the analysis presented above and in Section 4.3, it was assumed that k buildings from the set of m buildings collapsed, and consequently, the resilience index for the set of buildings was reduced accordingly (per Eq. (7)). However, this assumption does not consider the correlation between the probability of collapse between buildings in a community; i.e., the building that collapsed can result in partial or total collapse of nearby buildings. This condition is highly probable in dense urban environments, where the buildings are clustered close together. If p is defined as the number of buildings that collapsed over a non-collapsed building, the resilience index for the set of m identical buildings can be computed as:

$$RI = \left(1 - \frac{k+p}{m}\right)\left(\frac{\alpha(t_D + t_R) + \omega(0.5t_1 + t_{LL} + t_2) + 0.5\beta t_2}{t_D + t_R}\right) \quad (8)$$

In Eq. (8), p must be equal to or less than the smaller of *(m-k)* (number of non-collapsed buildings) and k (number of collapsed buildings). This means that the maximum number of non-collapsed buildings that can be affected should not be greater than the maximum number of k collapsed buildings. Also, Eq. (8) considers that any collapsed building can only induce total collapse in only one non-collapsed building. This assumption implies that when a building collapses, it neglects the possibility that this collapse could itself induce collapse in two or more adjacent buildings. For example, a scenario in which one building collapses and induces total collapse on one other building, and some damage in adjacent buildings, is not considered in Eq. (8) (although more sophisticated formulations that account for these effects could be implemented mathematically). Likewise, a "cascading" effect is not considered here either, whereby a cascading effect is produced when a building that collapses due to another building falling over, itself induces total collapse in an adjacent building, and so on, in a chain reaction (also cascading failures of buildings in urban centers have typically not been observed).

Note that Eq. (8) can also be expressed as:

$$RI = \left[1 - \frac{k}{m}(1+\gamma)\right]\left(\frac{\alpha(t_D + t_R) + \omega(0.5t_1 + t_{LL} + t_2) + 0.5\beta t_2}{t_D + t_R}\right) \quad (9)$$

where γ represents the percentage of buildings that collapsed over non-collapsed buildings from the k collapsed buildings. The value of γ varies between 0 and 1 for k/m less than or equal to 0.5. Fig. 10 presents the resilience indexes for a set of m buildings with different collapse percentages (k/m) and different values of γ, β and ω. For all the curves presented in Fig. 10, it was assumed that t_D, t_{LL}, t_1, and t_2 were 80, 35, 135, and 70 days, respectively. The values computed for α using Eq. (3) were also obtained for each curve. It can be observed that for higher α values, the resilience indexes decreased faster for the same γ value. As expected, this means that the collapse of a less damaged building (i.e., high α value) affects the resilience index of the community more considerably. Additionally, as γ increases, the resilience indexes for the set of m buildings decreased faster. It should be noted that only the curves for $\gamma = 0$ will converge to a zero-resilience index at a 100% collapse probability, the point at which all the curves in Fig. 7 converged. Based on the limits for γ, which are similar to the limits for p in Eq. (8), each different value of γ has a different collapse probability for a zero-resilience index.

Seismic resilience of building inventory

The analysis presented in Section 4.3 was applied to different sets of m identical buildings with resilience indexes computed using Equations Eq. (5) and Eq. (7). In this section, the same analysis is applied to communities formed by a set of m different buildings.

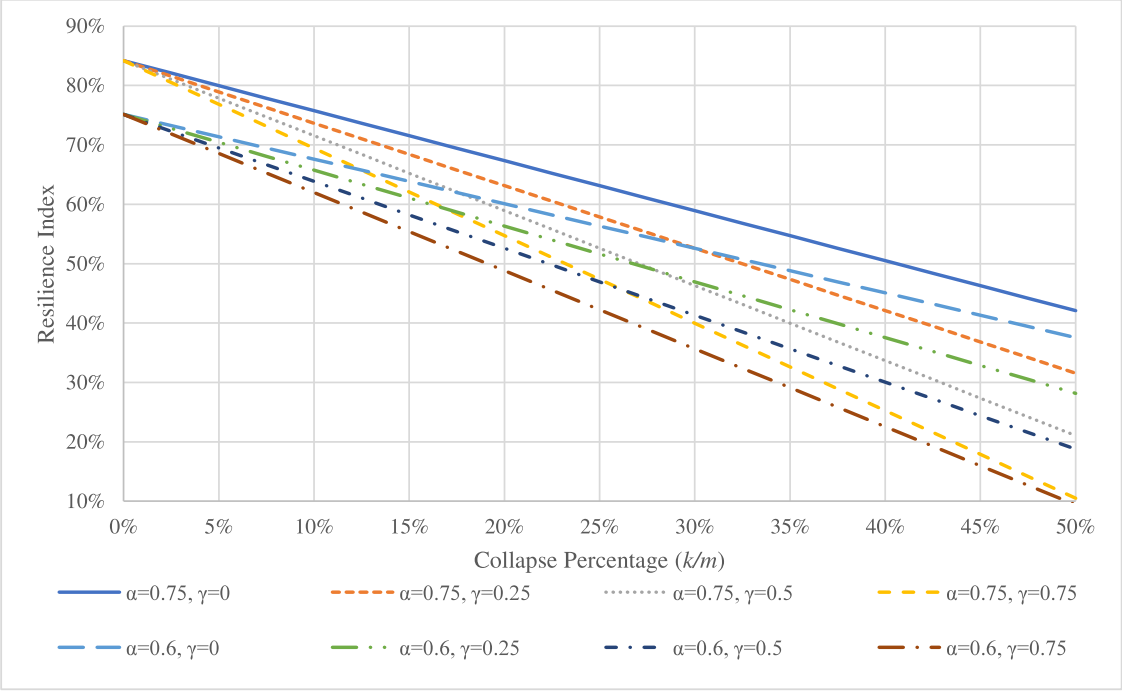

Fig. 10. Resilience indexes for a set of m buildings and different α and γ values.

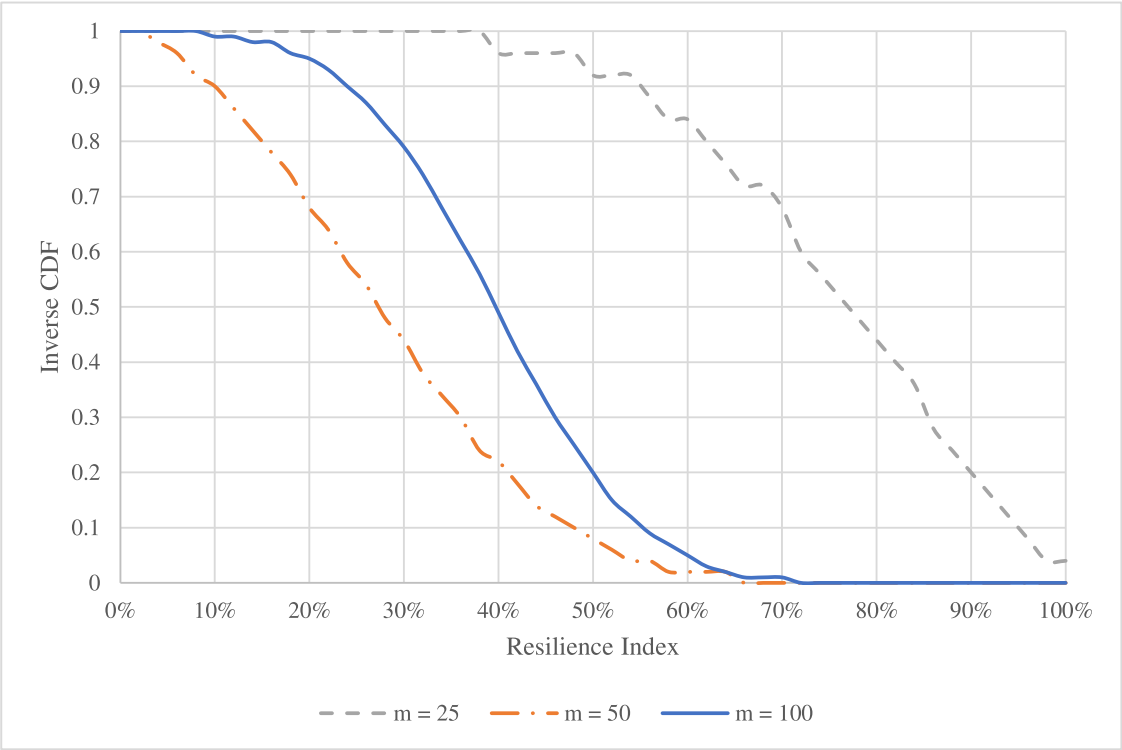

Fig. 11. Resilience indexes for different communities of m buildings.

The communities considered in this section includes the four example buildings used in this study (namely, Buildings (1) to (4)), together with a set of additional buildings having different characteristics (i.e., dimensions, structural systems, etc.). This resulted in a set of m buildings having a range of different resilience indexes in each community. Three different communities were considered. For expediency in directly illustrating the result of the process, instead of exactly calculating the resilience of m buildings using the above procedure, their resilience indexes have been randomly assumed. Fig. 11 presents the number of buildings in each community and how many of those buildings have resilience indexes greater than specific thresholds. For example, for Community 2 ($m = 50$), 11 buildings achieved resilience indexes greater than 40%, but only one of those 11 buildings achieved a resilience index greater than 60%. Note that for the examples presented here, it is considered that the three considered communities have enough contractors to perform the repairs in all the affected buildings simultaneously (i.e., repairs are performed in parallel). It is also assumed that the resilience indexes for each building already include their respective collapse probabilities.

Fig. 11 shows the inverse CDF for the resilience index of the buildings for each community. Evidently, as the number of buildings increases, the curves exhibit a "smoother" behavior. However, more importantly in this example, it can also be observed that, on average, Community 2 ($m = 50$) had lower resilience indexes, with a median building-resilience index of 27%. The community with 100 buildings ($m = 100$) achieved a median building-resilience index of 40%, while the community with 25 buildings ($m = 25$) was the one with the highest median building-resilience index of 77% and is therefore, by this measure, deemed to be the more resilient community.

A similar analysis as the one presented here, but applying the approaches developed in this work to obtain resilience indexes for each of the buildings that constitute a community (instead of artificially generating them as in the above example), would provide an important indicator of how resilient is the community in terms of its building stock. Additionally, this analysis would be helpful to identify "weak spots" or specific "deficiencies" in a given community.

Conclusion

On the basis of the work conducted here, it was found that for a small community, both loss of functionality and repair time influence the quantified resilience of buildings in a community. In that perspective, post-earthquake contractor availability to conduct the repair work is a critical factor on resilience assessment of the building inventory. Furthermore, it was observed that for the extreme scenario assuming that only one contractor was available to perform all the required repair works, the initial drop in building functionality has a significant influence on community resilience as the number of affected buildings in the community increases. Such a situation highlights well the importance of mitigating the risk of initial damage to achieve greater resilience in light of the challenges of finding labor when a large number of buildings simultaneously require repairs. Mitigation is important to improve the "robustness" dimension of resilience for buildings, which translates to a lower decrease in functionality after an adverse event.

It was shown that a building-resilience index could be defined and calculated for an entire community with a larger ensemble of buildings. The percentage of buildings having a resilience index greater than or equal to a specified threshold can be used to assess the overall resiliency of a given building inventory, evaluate "weak spots" in the community, and consequently, indicate where improvements are needed to increase the resilience of the community.

Declaration of interests

The authors declare that they have no known competing financial interests or personal relationships that could have appeared to influence the work reported in this paper.

Acknowledgments

This research was partly supported by the Fulbright Laspau Program, which granted the first author a scholarship. Any opinions, findings,

conclusions, or recommendations in this paper, however, are solely of the authors and do not necessarily reflect the views of the sponsors.

References

[1] Bruneau M, et al. A framework to quantitatively assess and enhance the seismic resilience of communities. Earthq Spectra 2003;19(4):733–52.

[2] Cimellaro GP, Solari D, Bruneau M. Physical infrastructure interdependency and regional resilience index after the 2011 Tohoku Earthquake in Japan. Earthq Eng. Struct Dyn 2014;43(12):1763–84.

[3] Bruneau M, Reinhorn A. Structural Engineering Dilemmas, Resilient EPCOT, and other Perspectives on the Road to Engineering Resilience. In: Gardini P, editor. Routledge Handbook of Sustainable and Resilient Infrastructure. Routledge; 2018. p. 70–93.

[4] Bruneau M, Reinhorn A. Exploring the concept of seismic resilience for acute care facilities. Earthq Spectra 2007;23(1):41–62.

[5] Cimellaro GP, Reinhorn A, Bruneau M. Seismic resilience of a hospital system. Struct Infrastruct Eng 2010;6(1–2):127–44.

[6] Fischer K, Hiermaier S, Riedel W, Haring I. Morphology dependent assessment of resilience for urban areas. Sustainability 2018;10(1800).

[7] C. Renschler, A. Frazier, L. Arendt, G.P. Cimellaro, A. Reinhorn, and M. Bruneau, “A framework for defining and measuring resilience at the community scale: the PEOPLES Resilience Framework,” 2010.

[8] FEMA, “Hazus,” 2017. https://www.fema.gov/flood-maps/products-tools/hazus.

[9] Center of Excellence for Risk-Based Community Resilience Planning, “IN-CORE (Interdependent Networked Community Resilience Modeling Environment),” 2020. http://resilience.colostate.edu/in_core/.

[10] Koliou M, Masoomi H, van de Lindt JW. Performance assessment of tilt-up big-box buildings subjected to extreme hazards: tornadoes and earthquakes. J Perform Constr Facil 2017;31(5).

[11] Lin P, Wang N. Building portfolio fragility functions to support scalable community resilience assessment. Sustain Resilient Infrastruct 2016;1(3–4):108–22.

[12] Cutter SL, Burton CG, Emrich CT. Disaster resilience indicators for benchmarking baseline conditions. J Homel Secur Emerg Manag 2010;7(1).

[13] Koliou M, van de Lindt JW, McAllister TP, Ellingwood BR, Dillard M, Cutler H. State of the research in community resilience: progress and challenges. Sustain Resilient Infrastruct 2018;5(3):131–51.

[14] Gardoni P. Routledge Handbook of Sustainable and Resilient Infrastructure. Routledge 2019.

[15] S. Taghavi and E. Miranda, “Response assessment of nonstructural building elements,” 2003.

[16] NIST, “Research Needs to Support Immediate Occupancy Building Performance Objective Following Natural Hazard Events,” Washington, 2018. [Online]. Available: doi:10.6028/NIST.SP.1224.

[17] Burton HV, Deierlein G, Lallemant D, Singh Y. Measuring the impact of enhanced building performance on the seismic resilience of a residential community. Earthq Spectra 2017;33(4):1347–67.

[18] Sharma N, Tabandeh A, Gardoni P. Resilience analysis: a mathematical formulation to model resilience of engineering systems. Sustain Resilient Infrastruct 2017;3(2):49–67 [Online]. Available. doi:10.1080/23789689.2017.1345257.

[19] Salado Castillo JG, Bruneau M, Elhami Khorasani N. Functionality measures for quantification of building seismic resilience index. Eng Struct 2021;253 [Online]. Available. doi:10.1016/j.engstruct.2021.113800.

[20] Cimellaro GP, Reinhorn A, Bruneau M. Framework for analytical quantification of disaster resilience. Eng Struct 2010;32(11):3639–49.

[21] FEMA, *P-58-1: seismic performance assessment of buildings - methodology*, Second. 2018.

[22] FEMA, *P-58-3: seismic performance assessment of buildings - supporting electronic materials and background documentation*, Third. 2018.

[23] Arup, *Resilience-based earthquake design initiative (REDi) rating system for the next generation of buildings*. 2013.

[24] Group CoStar, “LoopNet,” 2020. http://www.loopnet.com/(accessed Jul. 10, 2020).